Molecular Crystals and Liquid Crystals
Publication details, including instructions for authors and subscription information:
http://www.tandfonline.com/loi/gmcl20

Synthesis and Solvatofluorochromism Behaviors on Intramolecular Charge Transfer System of Novel D-π-A Dyes

Byung-Soon Kim [a c], Hyungwook Yu [a b] & Young-A Son [b]

[a] Graduate School of Environmental and Information Sciences, Yokohama National University, Hodogaya-ku, Yokohama, 240-8501, Japan

[b] Department of Advanced Organic Materials and Textile System Engineering, Chungnam National University, Daejeon, 305-764, Korea

[c] Seoul Regional Center, Defense Agency for Technology and Quality, Seoul, 130-010, Korea

Version of record first published: 02 Aug 2012.

To cite this article: Byung-Soon Kim , Hyungwook Yu & Young-A Son (2012): Synthesis and Solvatofluorochromism Behaviors on Intramolecular Charge Transfer System of Novel D-π-A Dyes, Molecular Crystals and Liquid Crystals, 563:1, 257-271

To link to this article: http://dx.doi.org/10.1080/15421406.2012.689733

Mol. Cryst. Liq. Cryst., Vol. 563: pp. 257–271, 2012

ISSN: 1542-1406 print/1563-5287 online
DOI: 10.1080/15421406.2012.689733

Synthesis and Solvatofluorochromism Behaviors on Intramolecular Charge Transfer System of Novel D-π-A Dyes

BYUNG-SOON KIM,[1,3] HYUNGWOOK YU,[1,2] AND YOUNG-A SON[2,*]

[1]Graduate School of Environmental and Information Sciences, Yokohama National University, Hodogaya-ku, Yokohama 240-8501, Japan
[2]Department of Advanced Organic Materials and Textile System Engineering, Chungnam National University, Daejeon 305-764, Korea
[3]Seoul Regional Center, Defense Agency for Technology and Quality, Seoul 130-010, Korea

Solvatochromic donor-π-acceptor (D-π-A) charge transfer dyes have been great attention from the viewpoint of their applicability as probes for the determination of solvent polarity and colorimetric chemosensors. In this work, novel solvatochromic fluorophore dyes based on D-π-A charge transfer system were designed and synthesized containing a strong electron-donating unit as a carbazole moiety and three different strong electron-withdrawing units. The corresponding molecular design and the optical properties of the D-π-A dyes were examined in various solutions with widely different polarity. The prepared dyes were found to exhibit a positive fluorescence solvatochromism. Furthermore, the energy properties of these dyes were also computationally optimized and calculated by computational simulation approaches using Material Studio 4.3 *and electrochemical measurement.*

Keywords Cyclic voltammetry; D-π-A charge transfer dye; molecular orbital calculations; optical property; positive fluorescence solvatochromism.

1. Introduction

Solvatochromism effect is characterized by color changing behaviors in a strong dependence of absorption or emission spectra for the dye chromophores with different solvents [1, 2]. The described behaviors of the solvatochromism depend on the differential stabilization of the ground and the excited states of the chromophore in the solvent polarity change. The differential stabilization of the ground and the excited states is corresponded with a change in the energy gap between these electronic states and consequently, with variations in Homo/Lumo position, intensity and shape of absorption or emission spectra can be

*Address correspondence to Prof. Young-A Son, Department of Advanced Organic Materials and Textile System Engineering, Chungnam National University, 220 Gung-dong, Yuseong-gu, Daejeon 305-764, Republic of Korea (ROK). Tel: (+82)42-821-6620; Fax: (+82)42-823-3736. E-mail: yason@cnu.ac.kr

determined. A significant spectral change in absorption or emission has attracted considerable attention as probes for the understanding of solvent polarity effects, colorimetric chemosensors and complex biological system [3–7].

Recently, many studies have focused on the solvatochromism effect and solvatochromic dyes such as pyrifinium betain [8] and stilbazolium [9] have been synthesized and studied. This effect was based on intramolecular charge transfer (ICT) system of molecular structure having donor-π-acceptor (D-π-A), and thus, the electron flowing within their molecular structures are considered to play a major role for the solvatochromism effect. These electron flowing effects of D-π-A charge transfer chromophoric system have also gained considerable importance from the viewpoint of their applications in optoelectronics materials [10–14]. There are many research activities [10–16] focused on the development for the power conversion efficiency, photo-stability and absorption or emission properties within their D-π-A structural systems. One of the key problems associated with the development for above mentioned application materials is to design the D-π-A structural system with high-performance properties.

In this study, we have designed and synthesized novel D-π-A charge transfer dyes by using carbazole moiety as a strong electro-donating unit and three different electro-withdrawing units such as malononitrile, 1-indanone, 1,3-indanedione. Cabazole derivative (**1**), namely 4-(9*H*-carbazol-9-yl)benzaldehyde, was easily synthesized by the reported procedure [17–19]. The designed novel D-π-A dyes (**2–4**) were synthesized by the one-step condensation of 4-(9*H*-carbazol-9-yl)benzaldehyde as a electron-donating unit with malononitrile for **2**, 1-indanone for **3**, and 1,3-indanedione for **4** as a electron-withdrawing unit, respectively. The solvatochromic behaviours on the effect of electro-withdrawing unit were investigated by UV-Vis absorption and fluorescent properties in several solvents with different polarity parameter in details. Their electronic states were also characterized by theoretical and electrochemical measurements.

2. Experimental

2.1 Materials and equipment

Cabazole (95%), potassium tert-butoxide (97%), malononitrile (99%), 1-indanone (99%) and 1,3-indanedione (97%) were purchased from Sigma-Aldrich Co. 4-fluorobenzaldehyde (98%) was obtained from Acros Organics Inc. Silica gel 60 (230-340 mesh, ASTM) was used for the column chromatography. The ^{1}H NMR spectra were recorded on a JNM-AL 400 MHz NMR instrument (JEOL Ltd.) with TMS as the internal standard. The elemental analyses were recorded on a Flash EA 1112 series (Thermo Fisher Scientific). The absorption and fluorescence spectra of the dyes were determined using an Agilent 8453 UV-Vis spectrophotometer and a Varian AT/Cary Eclipse Luminescence spectrophotometer, respectively. The concentration of the solutions used for absorption and fluorescence measurements was 1.0×10^{-5} M. Electron distributions and energy potentials were computationally calculated and optimized with *Material Studio 4.3*. The electrochemistry properties of these dyes were examined and determined on a *Versa STAT3* with three-electrode conventional electro chemical cell (a platinum wire served as a working electrode, an Ag/Ag+ electrode served as a reference electrode, and a carbon served as a counter electrode). Cyclic voltammetry (CV) test was conducted in an CH_2Cl_2 solution containing tetrabutlyammonium hexafluorophosphate electrolyte. The scan rate was set to 100mV/s. All measurements were taken at room temperature at approximately 298 K.

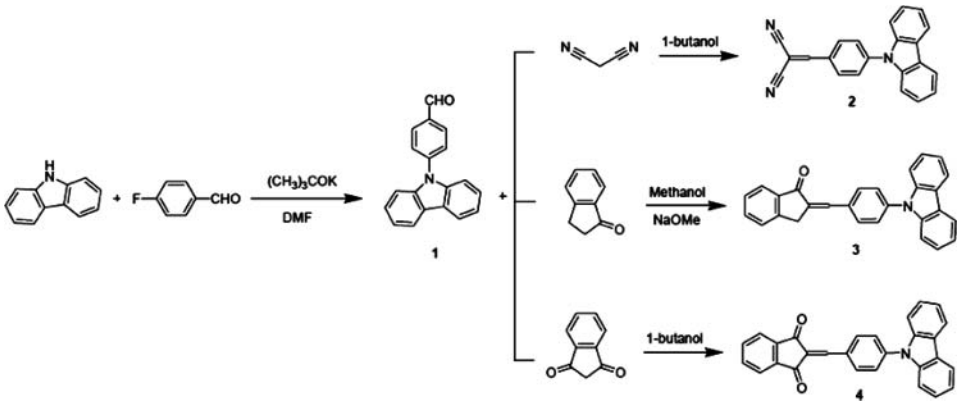

Scheme 1. Synthetic routes.

2.2 Synthesis and Characterization

As illustrated in Scheme 1, D-π-A dyes **2–4** were synthesized according to a previously described method with some modifications [20–23], and their chemical structure was confirmed by ^{1}H NMR and elemental analysis.

2.2.1 Donor unit 1. 4-(9*H*-carbazol-9-yl)benzaldehyde was synthesized by the reported procedure [17–19]. To the mixture of cabazole 50 mmol (8.40 g) and potassium tert-butoxide 50 mmol (5.60 g) were stirring in 200 ml DMF at 110°C. After 30 min, 4-fluorobenzaldehyde 50 mmol (6.20g) was added dropwise during the reaction. The resulting mixture was stirred for 36 h. After 36 h, the reaction was cooled to room temperature and the mixture was quenched into 1000 ml ice water. The mixed solution was stirring until the precipitate to be the enough. The solid was filtered and purified by recrystalization with acetone/ water (acetone:water = 10:1 *v/v*). Yield: 40.0% (4.00 g)

2.2.2 D-π-A dyes 2-4. Dye **2**, to 13 ml of 1-butanol was added a mixture of 2 mmol 4-(9*H*-carbazol-9-yl)benzaldehyde (0.54 g) and 2 mmol of the malononitrile (0.13 g) the resulting mixture was stirred. Reflux was continued for 8 h. After 8 h, the reaction mixture was cooled to room temperature. The precipitated crude product was filtered and then purified by recrytallization from 1-butanol. **2**, Yield: 67.0% (0.22 g); Anal. Calcd. For $C_{22}H_{13}N_3$: C, 82.74; H, 4.10; N, 13.16; Found: C, 82.99; H, 4.22; N, 12.41. ^{1}H NMR (CD_3COCD_3): 8.46(s, 1H), 8.38-8.36(d, 2H), 8.26-8.24(d, 2H), 8.01-7.98 (d, 2H), 7.64-7.61(t, 2H), 7.50-7.46(t, 2H), 7.37-7.35(t, 2H).

Dye **3**, 1-indanone 2 mmol (0.27 g) was dissolved in 20ml methanol. 4-(9*H*-carbazol-9-yl)benzaldehyde 2 mmol (0.54 g) and NaOMe (0.04g) dissolved in 10 ml of methanol was added and the reaction mixture was stirred at 40°C for 5 h. After 5 h, the reaction mixture was cooled to room temperature. The precipitated crude product was filtered and washed with distilled water. **3**, Yield: 58.0% (0.45 g); Anal. Calcd. For $C_{28}H_{19}NO$: C, 87.25; H, 4.97; N, 3.63; Found: C, 86.92; H, 5.01; N, 3.69. ^{1}H NMR (CD_3Cl_3): 8.26-8.25(d, 2H), 8.24-8.23(d, 2H), 8.15-7.81(m, 3H), 7.74-7.71(m, 3H), 7.55-7.45(m, 5H); 7.34-7.30(t, 2H), 4.28-4.27(s, 2H).

Dye **4**, 1.4 mmol of 1,3-indanedione (0.21 g) and 4-(9*H*-carbazol-9-yl)benzaldehyde (0.38 g) were dissolved in 15ml of 1-butanol. Reflux was continued for 3 h. After 3 h,

the reaction mixture was cooled to room temperature. The precipitated crude product was filtered and then purified by column chromatography using ethyl acetate/ *n*-hexane (ethyl acetate:*n*-hexane = 1:4 v/v). **4**, Yield: 37.0% (0.28 g); Anal. Calcd. For $C_{28}H_{17}NO_2$: C, 84.19; H, 4.29; N, 3.51; Found: C, 83.42; H, 4.53; N, 3.84. ^{1}H NMR (CD_3Cl_3): 8.69-8.67(d, 2H), 8.09-8.07(d, 2H), 8.00-7.97(m, 2H), 7.91(s, 1H), 7.80-7.76(m, 2H), 7.73-7.71 (d, 2H), 7.52-7.50(d, 2H), 7.40-7.35(t, 2H), 7.28-7.24(t, 2H).

2.3 Crystal Growth and Data Collection

Among the three D-π-A dyes, single yellow prism crystal of **2** and **3** suitable for X-ray diffraction measurement was grown by solvent diffusion method and solved by a direct method *SIR 92* [24] and *SIR 2004* [25] using the CrystalStructure [26] crystallographic software package. Details on the crystal structure of **2** will be discussed in elsewhere [27] and the experimental method and crystal structure of **3** have been published [28].

3. Results and Discussion

3.1 Solvatochromic Behaviours

We designed and synthesized the solvatochromic dyes by using the D-π-A charge transfer dye system. Among the different electron-donating units, carbazole was examined in this study. Carbazole was well known compound as a strong electron donor. All the prepared dyes **2-4** were successfully obtained by a one-step reaction condensing 4-(9*H*-carbazol-9-yl)benzaldehyde (**1**) with various electron-withdrawing units, and their chemical structures were confirmed by ^{1}H NMR, and elemental analysis. All the prepared dyes were obtained in yields of 37–67%.

The absorption spectra in different polarity solvents are given in Fig 1. Optical properties for **2** and **4** were measured in CCl_4, toluene, CH_2Cl_2, 1,2-dichloroethane, THF and ethyl acetate (EA), whereas **3** have a different solubility in which it showed good solubility with CH_2Cl_2, 1,2-dichloroethane, THF, EA, acetonitrile and DMSO, and thus these solvents are used. The synthesized **2-4** show strong absorption around 420 nm, 370 nm and 450 nm in various solvent polarities. All the dyes have a strong absorption band within the spectral range of 20 nm, despite having various solvent polarities. It is difficult to assure that this spectral change in various solvent polarities is the major reason for solvatochromism. This spectral shift within the range of 20 nm is might be caused by their different solubility and stability features in different solvents and consequently the spectral change holds a no remarkable consideration.

However, the spectral change of the fluorescence bands of all dyes is noteworthy. The fluorescence bands in various solvent polarities for **2-4** are illustrated in Fig. 2, where solvents are used that for their absorption spectra. In order to define the relation and dependence of the emission values of **2-4** versus $E_T(30)$ [29, 30] solvent polarity parameter, the corresponding patterns were also determined (Fig. 3). The fluorescence spectra were measured by using their maximum absorption peaks such as 420 nm for **2**, 370 nm for **3**, and 450 nm for **4**, respectively. In the case of fluorescence emission spectra, they are exhibited with a solvent effect where the emission maximum showed shifts with solvent polarity. These spectra extended from 472 nm (CCl_4) to 565 nm (CH_2Cl_2) for **2**, 486 nm (THF) to 544 nm (Acetonitrile) for **3**, and 489 nm (CCl_4) to 570 nm (1,2-dichloroethane) for **4**, respectively, which confirms a strongly allowed π–π^* transition energy with charge

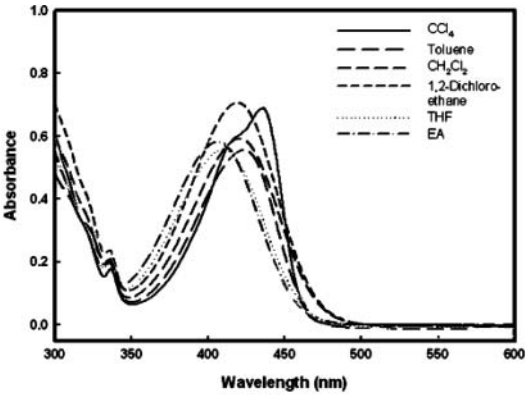

(a)

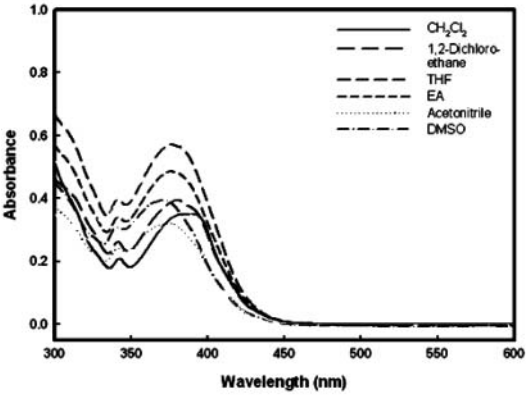

(b)

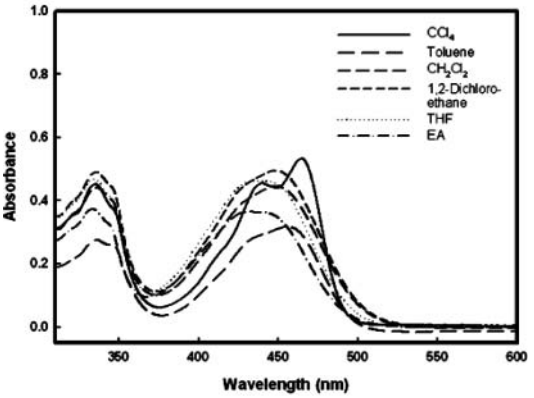

(c)

Figure 1. Absorption spectra of **2** (a), **3** (b), and **4** (c) in several solutions. The concentration of dyes is ca. 1.0×10^{-5} M.

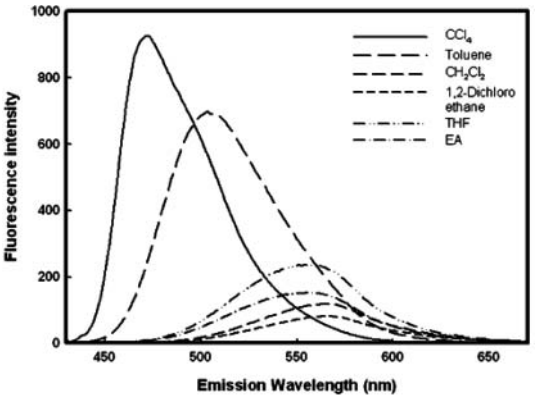

(a)

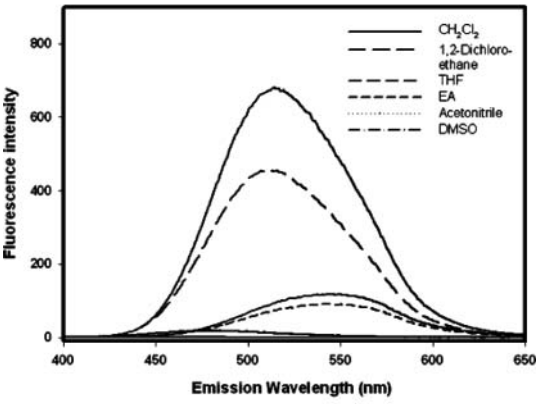

(b)

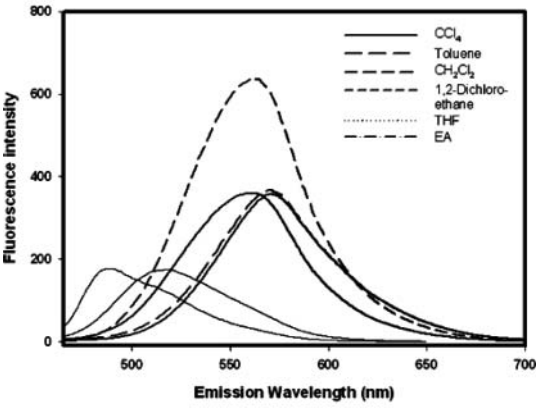

(c)

Figure 2. Fluorescence emission spectra of **2** (a), **3** (b), and **4** (c) in several solutions. The concentration of dyes is ca. 1.0×10^{-5} M.

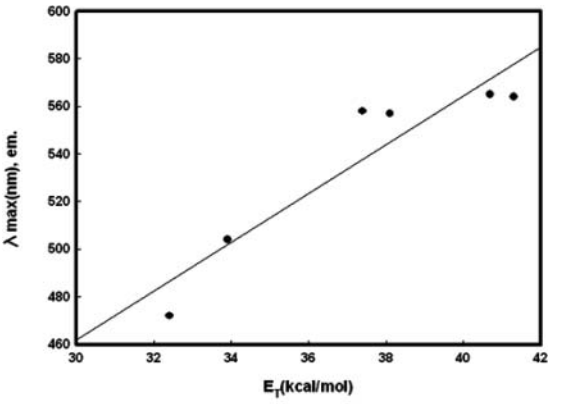

(a)

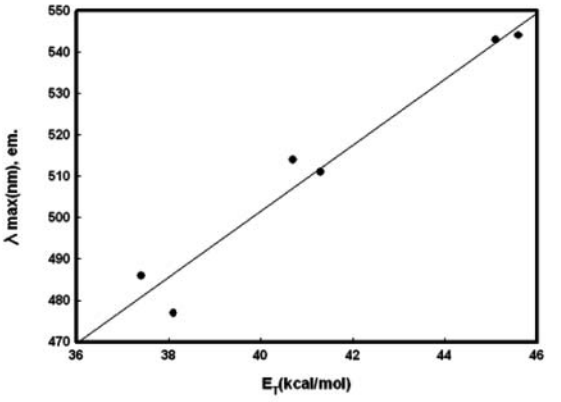

(b)

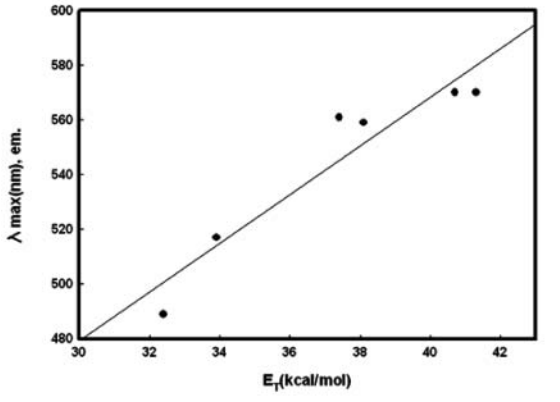

(c)

Figure 3. Plot of emission maxima of **2** (a), **3** (b), and **4** (c) versus solvent polarity parameter $E_T(30)$.

Table 1. $\lambda_{max,abs}$ and $\lambda_{max,em}$ values of **2**-**4** in various solvents and $E_T(30)$ values.

Solvent	2		3		4		$E_T(30)$/ kcal mol^{-1}
	λ_{max}/nm	λ_{em}/nm	λ_{max}/nm	λ_{em}/nm	λ_{max}/nm	λ_{em}/nm	
CCl_4	436	472	—	—	457	489	32.4
Toluene	423	504	—	—	448	517	33.9
THF	409	558	375	486	430	561	37.4
EA	406	557	372	477	423	559	38.1
CH_2Cl_2	420	565	376	514	440	570	40.7
1.2-dichloroethane	419	564	376	511	441	570	41.3
DMSO	—	—	376	543	—	—	45.1
Acetonitrile	—	—	368	544	—	—	45.6

transfer characters because of differential solvation of ground and excited states of the probe [7].

The observed bathochromic shifted fluorescence bands with increasing solvent polarity for **2**-**4** can be regarded as a positive fluorescence solvatochromism. These finding characteristics also clearly indicated that a bathochromic shift was observed with increasing application solvent polarity, which was a positive fluorescence solvatochromism. Fluorescence emission photographs of **2**-**4** in several solvents are shown in Fig. 4. The various fluorescent emissions in different polarity solvents for **2**-**4** can be easily observed by the naked eyes. In all dyes, however, their fluorescence intensity was decreased with increasing solvent polarity, which causes by the fluorescence quenching of aromatic hydrocarbons corresponded to have via radical ion formation with solvent polarity [31, 32]. As above mentioned spectral behavior results in various solvents and $E_T(30)$ values for all dyes are listed in Table 1.

Among the all dyes, **3** exhibited the strong fluorescence intensity. In the case of **3**, it has an one electron-withdrawing unit as a carbonyl group on its 2,3-dihydro-1*H*-indene ring and this reflects a slight difference between other dyes within their electron distribution. This result clearly indicates that it has a strong electron-pushing and -pulling effect between electron-donating and electron-withdrawing units and it consequently shows the strong fluorescence intensity compared to other dyes. This electron charge distribution in **2**-**4** according to a simple model is illustrated in Fig. 5, which show a strong migration of electron charge distribution.

3.2 Theoretical and Electrochemical Calculations

To gain further insight into the interpretation of the ICT process of **2**-**4**, their molecular geometry and electro properties such as HOMO and LUMO energy values were computed by the density function theory (DFT) with exchange correction functional of local density approximation (LDA) based on the Perdew-Wang (PWC) set. All the calculation approaches were performed with a *Material Studio 4.3* program package [33]. The optimized molecular geometry and electron distribution of the HOMO and LUMO energy level for **2**-**4** is illustrated in Fig. 6. The molecule of **2**-**4** has a D-π-A conjugation system from the electro-donating carbazole group to the electro-withdrawing malononitrile for **2**,

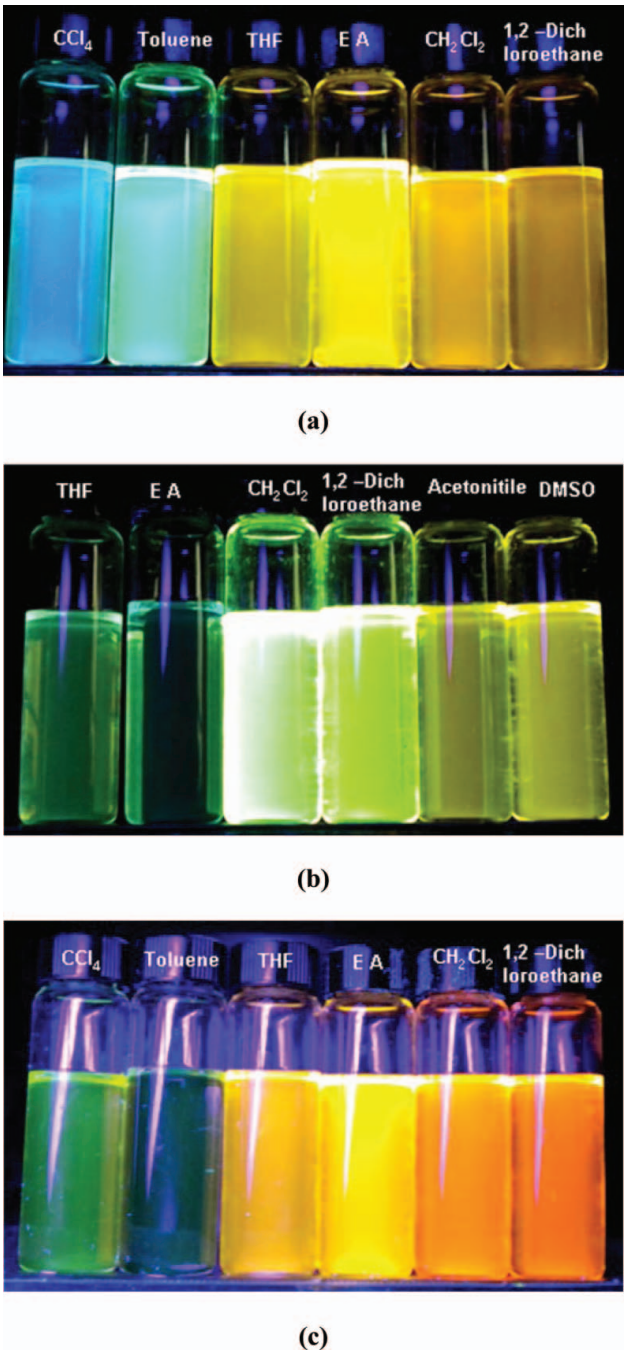

Figure 4. Fluorescence emission photographs of **2** (a), **3** (b), and **4** (c) in several solvents.

1-indanone for **3** and 1,3-indanedione for **4**, respectively. The electron distribution from HOMO to LUMO levels indicated a strong ICT character in these chromophoric dye systems upon excitation. In the case of **3**, HOMO-LUMO excitation moves from the amino nitrogen atom including carbazole moiety to an oxygen atom including 1-indanone moiety,

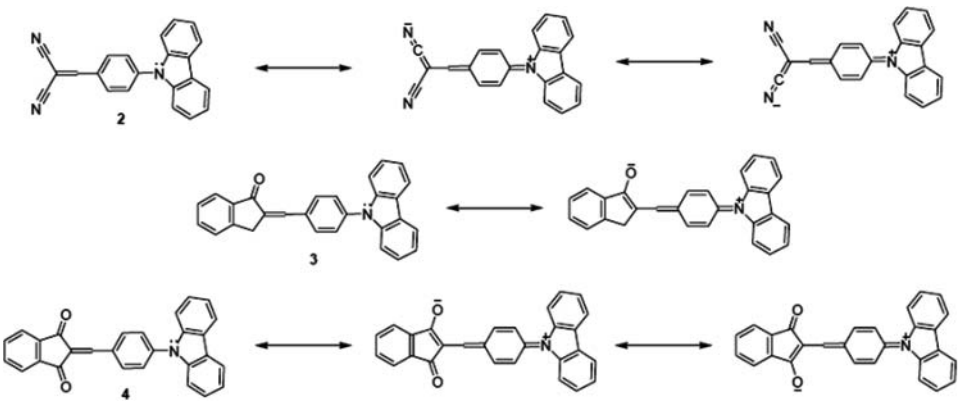

Figure 5. Electron-charge distribution in **2**-**4** according to a simple model.

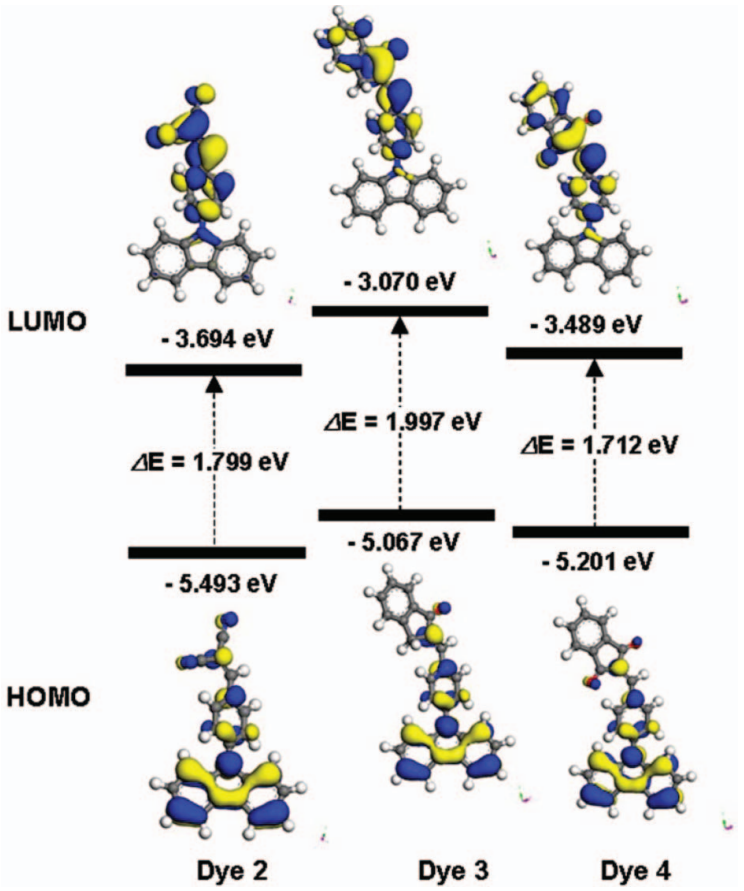

Figure 6. Optimized molecular geometry and electron distribution of the HOMO and LUMO energy levels for **2**-**4**.

whereas other dyes were mainly distributed over the two electro-withdrawing groups. This electron distribution strongly implies that a strong fluorescence intensity exhibits in **3** as described in solvatofluorchromism behaviors. This theoretical calculation result shows in good agreement with the obtained results from their optical properties in which **3** showed strong fluorescence intensity compared to other dyes.

Molecular orbital calculations were also performed with the electrochemical oxidation behavior by CV in CH_2Cl_2 solution containing tetrabutlyammonium hexafluorophosphate electrolyte at 100 mV/s of scan rate. Using this measurement, we can be determined the HOMO energy level using the electrochemical oxidation onset peak. The HOMO energy levels were calculated by the following formula (1) [34]:

$$\text{HOMO (eV)} = -4.8 - [\text{E}_{\text{peak or onset}} - \text{E}_{1/2}(\text{Ferrocene})] \quad (1)$$

where potential of E_{peak} and E_{onset} is the highest oxidation peak and rising starting peak potential, respectively. $\text{E}_{1/2}$(Ferrocene) denotes half-wave potential of Ferrocene (0.42 V). Among the two different approaches, we estimated the energy levels of **2**-**4** by onset approach. In addition, LUMO energy level was estimated with energy gap (ΔE) by using onset approach on their absorption spectra. The following equation (2) can be used at ΔE determination [34].

$$\Delta\text{E(eV)} = 1240/\lambda_{\text{oneset}} \quad (2)$$

As shown in Fig. 7, all dyes exhibited oxidation peak around and thus we have successfully found the oxidation onset peak at 0.61 V for **2**, 0.59 V for **3**, and 0.60 V for **4**, respectively. From the above equation (1), the ionization potentials (HOMO levels) were estimated to be -4.99 eV for **2**, -4.97 eV for **3**, and -4.98 eV for **4**, respectively. In addition, their LUMO energy levels were also estimated by the equation (2) to be -2.32 eV for **2**, -2.04 eV for **3**, and -2.48 eV for **4**, respectively. Dyes **2**-**4** caused ICT in their molecular conformation. Especially **3** had a strong effect within the D-π-A conjugation system and consequently strong fluorescence intensity was exhibited in **3**. Electrochemical results were also in good agreement with their observed optical and computational simulation features. The estimated potential electronic states (HOMO/ LUMO energy levels) by using electrochemical behavior and absorption spectra were also in similar characteristic pattern with their theoretical results and these compare results are also listed in Table 2.

Table 2. Optimized and calculated molecular orbital by theoretical and electrochemical method for **2**–**4**

	Computationally calculated			Determined with cyclic voltammetry		
Dye	HOMO/eV	LUMO/eV	ΔE/eV	HOMO/eV	LUMO/eV	ΔE/eV
2	−5.493	−3.694	1.799	−4.99	−2.32	2.62
3	−5.067	−3.070	1.997	−4.97	−2.04	2.93
4	−5.201	−3.489	1.712	−4.98	−2.48	2.50

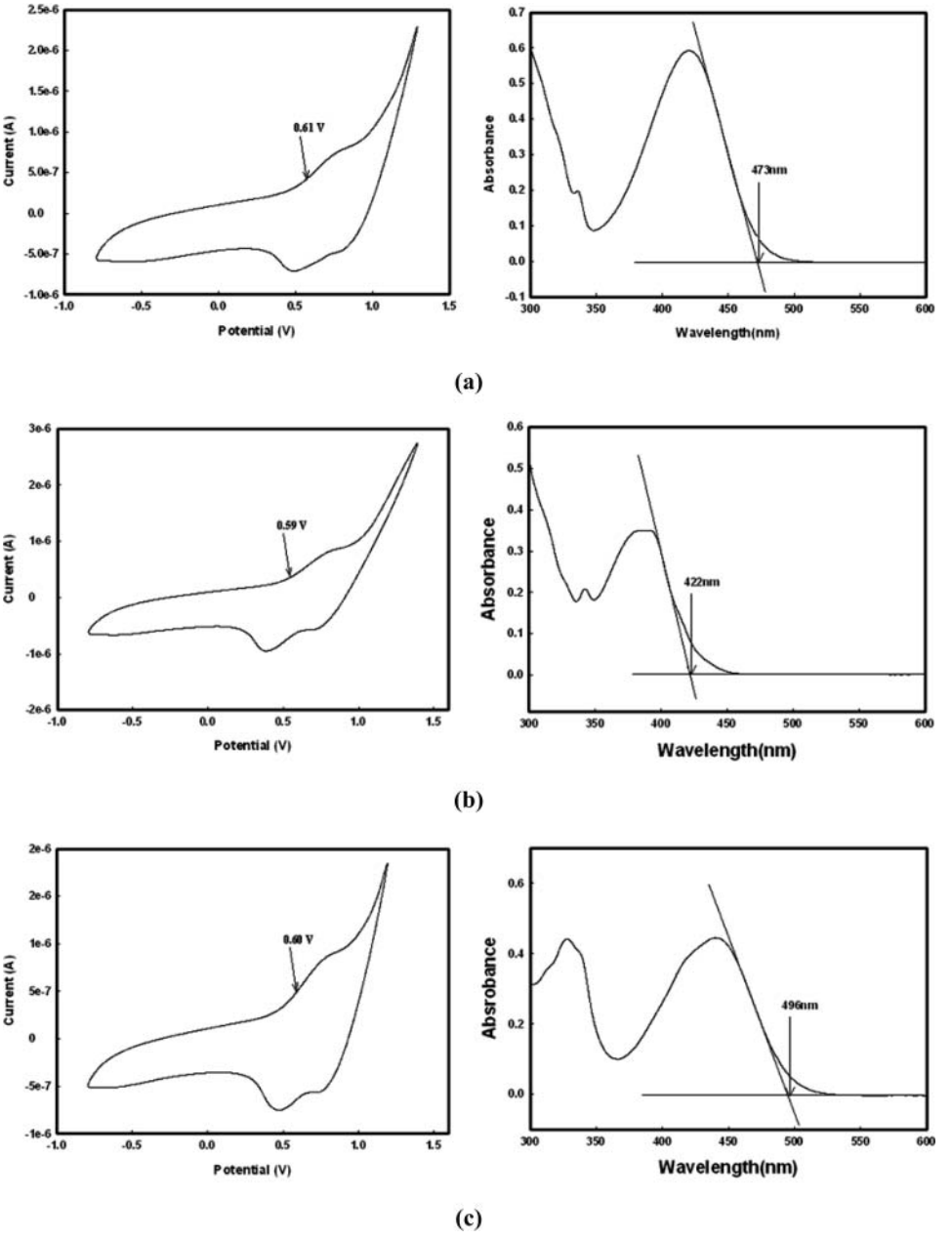

Figure 7. Electrochemical properties and absorption edge of **2** (a), **3** (b), and **4** (c) in CH_2Cl_2.

3.3 Molecular Structure of 2 and 3

Among the three D-π-A dyes, yellow crystal of **2** and **3** was successfully grown by solvent diffusion method and their details of crystal data collection and structure refinement parameters is listed in Table 3.

Table 3. Crystallographic and structure refinement data

Crystal data	dye 2	dye 3
Crystal size (mm)	0.40,0.10,0.04	0.30,0.10,0.10
Chemical formula	$C_{22}H_{13}N3$	$C_{28}H_{19}NO$
Formula weight (g mol^{-1})	319.36	385.46
Temperature (K)	296.1	296.1
Crystal system	Orthorhombic	Monoclinic
Space group	$P2_12_12_1$	$P2_1$/a
a (Å)	8.8010(2)	7.7107(3)
b (Å)	22.9945(6)	32.422(1)
c (Å)	24.7542(6)	8.3715(4)
α, (°)	90	90
β, (°)	90	105.095(3)
γ, (°)	90	90
V (Å^3)	5009.6(2)	2020.6(1)
Z	12	4
D_X (g cm^{-3})	1.270	1.267
μ (mm^{-1})	0.596	0.596
F (000)	808	808
$\boldsymbol{T}_{\min}$	0.721	0.713
$\boldsymbol{T}_{\max}$	0.976	0.942
No. of refln measured	47716	18287
No. of unique refrections	9135	3674
No. of parameters	676	290
$\theta_{\min}$ (°)	68.14	68.23
R_1, wR	0.0789,0.2179	0.0355,0.0711
GOF	0.929	0.862
$\Delta\rho_{\max}$, $\Delta\rho_{\min}$ (e Å^{-3})	0.15, −0.20	0.32, −0.36

Molecular conformation of **2** and **3** has almost planar structure between the electron-donating amine group and the electron-withdrawing malononitrile for **2** [27], 1-indanone for **3** [28]. Furthermore, their effective π-conjugation system developed between the electro-donating and the electro-withdrawing groups clearly recognized by their small bond alternation in the electro-withdrawing groups [35]. This finding indicated that **2** and **3** can move of electron smoothly in molecules and consequently these dyes are expected to exhibit the solvatochromism effect.

4. Conclusions

For gaining novel D-π-A charge transfer chromophoric dyes with the high-performance properties, we designed and synthesized based on a cabazole moiety as a strong electron-donating unit and three different electron-withdrawing units such as malononitrile, 1-indanone, 1,3-indanedione. In various solvent polarities, all the dyes significantly can be monitored in fluorescence emission bands within the spectral range of 70 nm, whereas no significant difference was observed in absorption bands. The fluorescence spectra exhibited a solvent effect where the emission maximum showed bathochromic shift with

solvent polarity. All dyes can be characterized as a positive fluorescence solvatochromism. Among the all dyes, **3** has strong fluorescence intensity due to its electron charge distribution in molecular structure. This electron distribution feature was confirmed their ICT by theoretical simulation approach and the calculation result were in good interpretation of their theoretical results. Furthermore, effective D-π-A conjugation system between the electron-donating and the electron-withdrawing groups of **2** and **3** was clearly recognized in molecular structure.

Acknowledgement

This research was supported by the Basic Science Research Program through the National Research Foundation of Korea (NRF) funded by the Ministry of Education, Science and Technology (No. 20110022326). This research was supported by a grant from the Fundamental R&D Program for Core Technology funded by the Ministry of Knowledge Economy, Republic of Korea.

References

[1] Reichardt, C. (1994). *Chem. Rev.*, *94*, 2319.
[2] Banerjee, D., Laha, A. K., & Bagchi, S. (1995). *Indian J. Chem. A*, *34*, 94.
[3] Masternak, A., Wenska, G., Milecki, J., Skalski, B., & Franzen, S. (2005). *J. Phys. Chem A*, *109*, 759.
[4] Hassanzadeh, A., Loghmani-Kjouzani, H., Sadeghi, M. M., & Mehrabi, H. (2007). *Spect. Acta. A*, *67*, 105.
[5] Sung-Hoon Kim, Sue-Yoen Lee, Seon-Yeong Gwon, Young-A Son, & Jin-Seok Bae, (2010). *Dyes and pigments*, *84*, 175.
[6] Yong-A Son, Seon-Yeong Gwon, Sue-Yoen Lee, & Sung-Hoon kim, (2010). *Spect. Acta. A*, *75*, 225.
[7] Rurack, K., Bricks, J. L., Reck, G., Radeglia, R., & Resch-Genger, U. (2000). *J. Phys,Chem A*, *104*, 3087.
[8] Reichardt, C., Andreas, Röchling, & Gerhard Schäfer. (2003). *J. Phys. Org. Chem.*, *16*, 682.
[9] Benjamin J., Coe, James, A. Harris, Jonathan J. Hall, Bruce S. Brunschwig, Sheng-Ting Hung, Wim Libaers, Koen Clays, Simo J. Coles, Peter N. Horton, Mark E. Light, Michael B. Hursthouse, Javier Garin, & Jesus Orduna. (2006). *Chem. Mater.*, *18*, 5907.
[10] Giedre Bubniene, Tadas Malinauskas, Maryte Dackeviciene, Vygintas Jankauskas, & Vytautas Getautis. (2010). *Tetrahedron*, *66*, 3199.
[11] Wai-Yeung Wong, & Cheuk-Lam Ho. (2009). *J. Mater. Chem.*, *19*, 4457.
[12] Walzer, K., Maennig, B., Pfeiffer, M., & Leo, K. (2007). *Chem. Rev.*, *107*, 1233.
[13] Christos, D. Dimitrakopoulos, & Patrick R. L. Malenfant. (2002). *Adv. Mater.*, *14*, 99.
[14] Afshin Hadipour, Bert de Boer, & Paul W. M. Blom. (2008). *Adv. Funct. Mater.*, *18*, 169.
[15] Antonov, V. S., & Hohal, K. L. (1983). *Appl. Phys. B*, *32*, 9.
[16] Prasanna de Silva, A., Nimal Gunaratne, H. Q., Thorfinnur Gunnlaugsson, Allen J. M. Huxely, Colin P. McCoy, Jude T. Rademacher, & Terence E. Rice. (1997). *Chem. Rev.*, *97*, 1515.
[17] Xiqi Zhang, Zhenguo Chi, Zhyyong Yang, Meina Chen, Bingjia Xu, Lin Zhou, Chengcheng Wang, Yi Zhang, Siwei Liu, & Jiarui Xu. (2009). *Opt. mater.*, *32*, 94.
[18] Hongxia Shao, Xiaopeng Chen, Zixing Wang, & Ping Lu. (2007). *J. Lumin*, *127*, 349.
[19] Jie-Ying Wu, Yue-Li Pan, Xuan-Jun Zhang, Tao Sun, Yu-Peng Tian, Jia-Xiang Yang, & Zhong-Ning Chen. (2007). *Inorg. Chim. Acta*, *360*, 2083.
[20] Xiaochuan Li, Sung-Hoon Kim, & Young-A Son. (2009). *Dyes and Pigments*, *82*, 293.
[21] Horie, S., Nagata, M., & Nakano, J. (1984). *United States Patent*, US 4469678.
[22] Murakami, M., Fukuyama, M., Suzuki, M., & Hashimoto, M. (1996). *Japanese Kokai Tokkyo Koho*, JP 08097465.

[23] Kato, E. (2004). *Japanese Kokai Tokkyo Koho*, JP 2004042381.
[24] Altomare, A., Cascarano, G., Giacovazzo, C., Guagliardi, A., Burla, M. C., Polidori, G., & Camalli, M. (1994). *J. Appl. Cryst.*, *27*, 435.
[25] Burla, M. C., Caliandro, R., Camalli, M., Carrozzini, B., Cascarano, G. L., De Caro, L., Giacovazzo, C., Polidori, G., & Spagna, R. (2005). *J. Appl. Cryst.*, *38*, 381.
[26] Crystal Structure 3.8: Crystal structure analysis package, *Rigaku and Rigaku/MSC*, The Woodlands, TX (USA), pp. 1998–2007.
[27] Byung-Soon Kim, Su-ho Kim, Shinya Matsumoto, & Young-A Son. Unpublished results.
[28] Byung-Soon Kim, Su-Ho Kim, Shinya Matsumoto, & Young-A Son. (2011). *Z. Kristallogr. NCS*, *226*, 177.
[29] Reichardt, C. (2003). 3rd ed., Weinheim, Wiley-VCH.
[30] Reichardt, C. (1994). *Chem. Rev.*, *94*, 2319
[31] Khalide E. Al-Ani, & M. Al-Sabti. (1983). *J. Phys. Chem.*, *87*, 446.
[32] Yan Lin, Jingrong Chen, Puhui Xie, Jianhua Wang, Yuanjun Hou, Lianqi Zhang, Baowen Zhang, & Yi Cao. (2000). *Res. Chem.* Intermed., *26*, 793.
[33] Delley, B. (2000). *J. Chem Phys.*, *113*, 7756.
[34] Lee, H. S., & Kim, J. H. (2007). *Polymer science and Technology*, *18*, 488.
[35] Frank H. Allen, Olga Kennard, David G. Watson, Brammer, L., Guy Orpen, A.,& Robin Taylor. (1987). *J.Chem. Soc. Perkin Trans.* 2, S1.